Scatterometry control for multiple electron beam lithography

Yoann Blancquaert [a], Nivea Figueiro [b], Thibault Labbaye [a], Francisco Sanchez [b], Stephane Heraud [b], Roy Koret [c], Matthew Sendelbach [d], Ralf Michel [b], Shay Wolfling [c], Stephane Rey [a], Laurent Pain [a]
[a] CEA-LETI, Minatec Campus, 17 rue des Martyrs Grenoble, 38054 Cedex9, France
[b] Nova Measuring Instruments, GmbH, Moritzburger Weg 67 01109, Dresden, Germany
[c] Nova Measuring Instruments, LTD, P.O. Box 266, Weizmann Science Park, Rehovot 76100, Israel
[d] Nova Measuring Instruments, Inc., 2055 Gateway Place, Ste. 470, San Jose, CA 95110, USA

ABSTRACT

The evaluation of scatterometry for monitoring intended variations in innovative scatterometry targets that mimic non-uniformities potentially caused by multibeam Maskless Lithography (MEB-ML2) is presented. Specialized scatterometry targets consisting of lines and spaces were produced that have portions exposed using the nominal, or POR (Process of Record), dose, and portions exposed with a slightly different dose. These exposure plans created targets with different line CDs (critical dimensions). Multiple target designs were implement, each with a different combination of magnitude of CD shift and size of the region containing lines with a shifted CD. The scatterometry, or OCD (Optical Critical Dimension), spectra show clear shifts caused by the regions with shifted CD, and trends of the scatterometry results match well with trends of the estimated CD as well as the trends produced by measurements using a critical dimension scanning electron microscope (CD-SEM) system. Finally, the OCD results are correlated to the CD-SEM measurements. Taking into account resist morphology variations across the wafer, correlations between OCD and CD-SEM of the weighted average CD across the various targets are shown to be very good. Correlations are done using the rigorous TMU analysis methodology. Due to the different targeted CD values within each scatterometry structure, a new methodology for estimating the error of the CD-SEM measurements for nominally non-uniform targets is presented.

Keywords: scatterometry, alternative lithography, e-beam lithography, multibeam, multiple e-beam, dose variation, TMU, TMU analysis

1. INTRODUCTION

In the past few years, several different alternative patterning strategies have been investigated. Some examples are Extreme Ultraviolet Lithography (EUVL), Directed Self-Assembly (DSA), Nanoimprint Lithography (NIL), Sidewall Image Transfer (SIT) and e-beam Maskless Lithography (EB-ML2). Each of these alternatives present their own specific advantages and challenges, many of which differ from the ones encountered with traditional photolithography. While the industry has developed approaches to evaluate, monitor and control optical lithography processes, methods for the more recent alternative patterning strategies are still being developed. Example challenges among the alternative strategies include pitch walking for the SIT method, residual resist underneath the pattern for NIL, and beam variation for multibeam lithography. Each of these challenges demands a metrology or inspection technique capable of meeting the specified requirements for monitoring and control. For multibeam Maskless Lithography, beam to beam variation can consist of changes or differences in beam dose and beam registration[1]. In order to monitor and eventually control such variations, a non-destructive, high throughput, precise, and accurate metrology method is required.

Although scatterometry is commonly used in semiconductor development and manufacturing for measuring periodic structures that are often complex, it has also been shown to successfully measure patterning variation levels of non-periodic structures[2]. This ability to detect undesired, non-periodic patterning variations across large regions (tens of microns across) makes scatterometry appealing for the detection of local patterning variability within a large array of multibeam-patterned structures.

Metrology, Inspection, and Process Control for Microlithography XXXI, edited by Martha I. Sanchez, Vladimir A. Ukraintsev
Proc. of SPIE Vol. 10145, 101451F · © 2017 SPIE · CCC code: 0277-786X/17/$18 · doi: 10.1117/12.2261389

Downloaded From: http://proceedings.spiedigitallibrary.org/ on 04/30/2017 Terms of Use: http://spiedigitallibrary.org/ss/termsofuse.aspx

The present work evaluates methodologies for monitoring multibeam dose variation through the use of scatterometry measurements of innovative target designs. The targets are designed to mimic dose variation in multiple e-beam lithography so that such variation can be monitored and minimized.

2. STRUCTURE AND DESIGN

The film stack of the wafers used in this work consists of patterned e-beam resist on top of an Anti-Reflective Coating and a Spin-on Carbon (SoC) hard mask (figure 1).

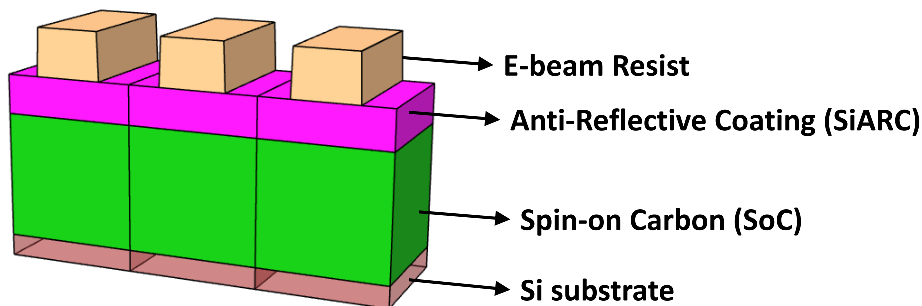

Figure 1: Film stack used in this work.

The e-beam tool used to pattern the wafer was used in a manner to mimic how a multibeam tool at CEA-LETI[3,4] might pattern a wafer: by exposing each 50x50 µm scatterometry target in 25 stripes, each 2 µm wide and 50 µm long. The scatterometry target array designed for this work is shown in Figure 2; controlled variations are induced inside the targets. The target array has built-in DOE conditions: the rows (0 – 7) indicate the number of beams (or stripes) affected, while the columns indicate the magnitude of the dose shift, but measured in nm.

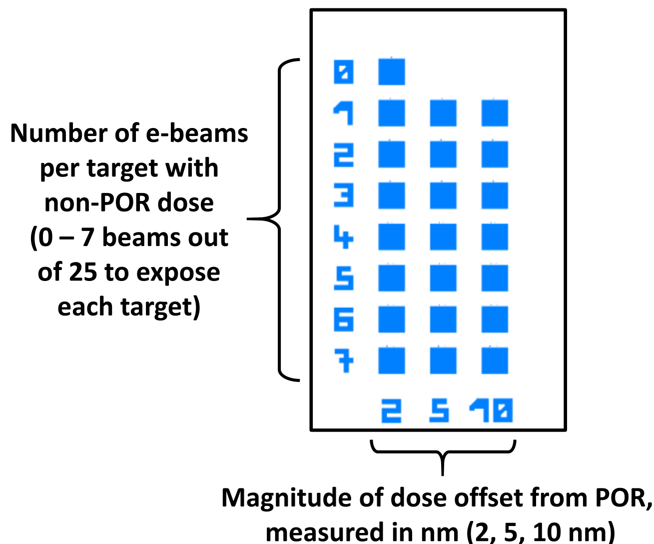

Figure 2: The scatterometry target array used in this work. This set of 22 targets is replicated 9 times across the wafer.

Figure 3 highlights the POR target, located in the upper left of the target array, where there are no beams/stripes exposed differently than POR. In contrast, figure 4 shows the layout of the targets with 1 non-POR beam exposure: a single 2 µm-wide stripe in the center of the target with a non-POR dose—one to produce lines with a CD offset of 2, 5, or 10 nm, depending on the OCD target within the row. The regions to either side of the non-POR stripe are exposed as POR.

Downloaded From: http://proceedings.spiedigitallibrary.org/ on 04/30/2017 Terms of Use: http://spiedigitallibrary.org/ss/termsofuse.aspx

Finally, figure 5 shows the layout of the targets with 7 non-POR beam exposures. Together, these make up a 14 µm-wide non-POR stripe in the target, again with POR regions on either side. Thus, targets closer to the bottom of the scatterometry array have a greater portion of their area covered by non-POR regions, compared to targets closer to the top of the array.

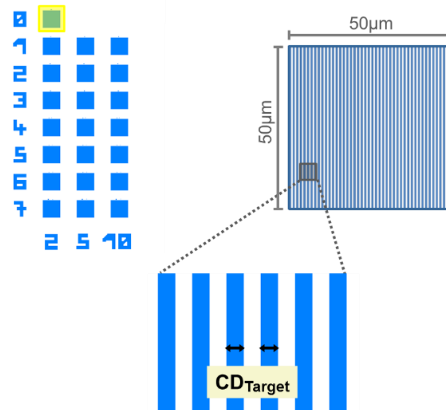

Figure 3: The POR target, located in the "0th row" of the scatterometry array, is made of 25 stripes, each 2 µm wide, that have been exposed with the POR dose.

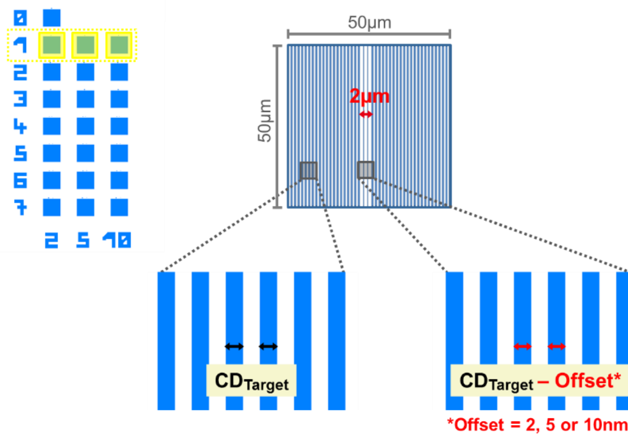

Figure 4: The targets in row 1 have a single 2 µm-wide stripe that has been exposed with a non-POR dose.

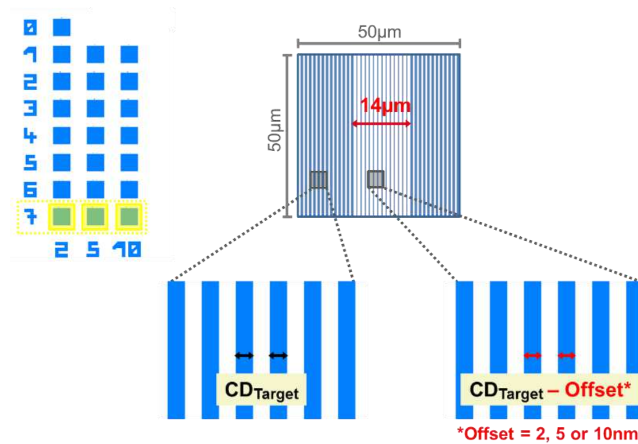

Figure 5: The targets in row 7 have seven 2 µm-wide stripes (totaling 14 µm in width) that have been exposed with a non-POR dose.

Downloaded From: http://proceedings.spiedigitallibrary.org/ on 04/30/2017 Terms of Use: http://spiedigitallibrary.org/ss/termsofuse.aspx

3. TMU ANALYSIS AND SAMPLING

3.1 Overview of TMU analysis

TMU (Total Measurement Uncertainty) analysis[5,6,7] was originally developed to be a type of calibration exercise where measurements from a Tool under Test (TuT) could be calibrated to those of a Reference Measurement System (RMS). The results of the analysis could then be used to rescale the TuT measurements to the scale of the RMS; that is, the rescaled TuT measurements would have a linear correlation with unity slope and zero offset when plotted against the RMS measurements. Its most common use now, however, is to assess both relative accuracy and precision by combining them into a single meaningful metric. Here, relative accuracy is defined as the ability of one measurement method to track changes in a measured parameter when compared to another measurement method, while being insensitive to changes in other parameters and unaffected by the average offset between the methods.

TMU analysis computes the total error (scatter) in a correlation between measurements from the TuT and the RMS, and states that this total error is the sum of two terms, one of which is associated with the TuT and the other is associated with all other errors:

$$\hat{\sigma}^2_{Mandel} = \hat{\sigma}^2_{TuT} + \hat{\sigma}^2_{RMS} \tag{1}$$

where $\hat{\sigma}^2_{Mandel}$ is the total error (also called the Mandel variance), $\hat{\sigma}^2_{TuT}$ is the error associated with the TuT, and $\hat{\sigma}^2_{RMS}$ is the compilation of all other errors, most notably those errors associated with the RMS. Note that each term is in variance form. Equation 1 can be rewritten into one form of the definition of TMU:

$$TMU \equiv 3\sqrt{\hat{\sigma}^2_{Mandel} - \frac{RMSU^2}{9}} \tag{2}$$

where

$$TMU = 3\hat{\sigma}_{TuT} \tag{3}$$

and

$$RMSU \equiv 3\hat{\sigma}_{RMS} \tag{4}$$

are the 3σ form of the errors associated with the TuT (TMU) and the compilation of all other errors (RMSU, or Reference Measurement System Uncertainty), respectively. The "hat" symbol over the sigmas indicates that these are estimated quantities; that is, they are estimates of associated "true" quantities that could be determined under ideal conditions, such as an infinite sampling size. Although other quantities in this work are also estimated, such as TMU and RMSU, for brevity purposes they are not given "hat" symbols. Besides the TMU and slope of the best-fit line, another important metric is the average offset:

$$average\ offset \equiv \bar{x} - \bar{y} \tag{5}$$

where $\bar{x}$ is the average of the TuT measurements and $\bar{y}$ is the average of the RMS measurements.

3.2 Advantages of TMU analysis

Different methods are used among semiconductor metrologists to determine accuracy, but one of the most common methods is Ordinary Least Squares (OLS) regression, where the accuracy metric is R^2. TMU analysis has many advantages over OLS regression and the R^2 metric, including the use of units in TMU analysis. Having an accuracy metric

Downloaded From: http://proceedings.spiedigitallibrary.org/ on 04/30/2017 Terms of Use: http://spiedigitallibrary.org/ss/termsofuse.aspx

with units matching those of the measurement parameter makes it easy to apply specifications (specs). TMU analysis also is not nominally affected by the range of the data, so comparisons across different data sets and applications are straightforward. TMU analysis takes into account the error of the RMS. This is not done with OLS regression, yet in the semiconductor industry the RMS can often be a significant contributor to the scatter when compared to the TuT. Finally, TMU analysis computes meaningful upper and lower confidence limits. Typically, no confidence limits are calculated with OLS regression.

3.3 Most common form of RMSU

The most commonly used form of RMSU is described by Sendelbach *et. al.*[8] as "case #1" and occurs when at least 2 measurements per sample are made by the RMS. If the TuT probe size is relatively large compared to the RMS probe (such as when a scatterometry measurement is compared to a CD-SEM measurement), it is preferable to spread out the multiple small probe RMS measurements as evenly as possible across the measurement collection area of the TuT. This form of RMSU can be expressed as

$$RMSU = 3\sqrt{\frac{\overline{V}_S}{\overline{n}_S}} = 3\sqrt{\frac{\sum_{i=1}^{N_S}(V_S)_i}{\sum_{i=1}^{N_S}(n_S)_i}} \tag{6}$$

where $(V_S)_i$ is the variance of the RMS measurements for the ith sample, $\overline{V}_S$ is the average of those variances, $(n_S)_i$ is the number of RMS measurements for the ith sample, $\overline{n}_S$ is the average number of RMS measurements per sample, and N_S is the total number of samples.

3.4 TMU analysis for nominally non-uniform samples

There is no known prior instance in which TMU analysis was performed on data involving small probe RMS measurements of non-uniform samples, as is the case in this work. Thus, careful consideration had to be taken to ensure that the data collection and analysis was done correctly. Equation 6 assumes that the small probe RMS measurements are evenly distributed across the sample. In practice, metrologists cannot always ensure this—but any non-uniformities in RMS sampling are inconsequential when the across-sample variation is small, or when the "characteristic periodicity" of that variation is small compared to the typical distance between RMS sampling locations. Because the samples (scatterometry targets) in this study had significant non-uniformities in the measurement parameter of interest, however, the correct (and uniform) placement of these RMS measurements was more important than usual. CD-SEM measurement locations, 28 per target, were distributed in the region of the target where the OCD measurement spot was placed—so no CD-SEM measurements were collected near the edge of the target. The number of CD-SEM reference measurements per target was chosen in order to increase the likelihood that the RMSU remains smaller than the TMU, a practice promoted by Sendelbach *et. al.*[5] Furthermore, the CD-SEM measurement locations were roughly evenly distributed throughout this region—so for OCD targets that had a larger non-POR, or error, region, a greater proportion of the CD-SEM measurements were collected from that region, as compared to OCD targets with a smaller error region. An example of the placement of the CD-SEM measurement locations for the targets with three beams/stripes of non-POR dose is shown in figure 6.

Downloaded From: http://proceedings.spiedigitallibrary.org/ on 04/30/2017 Terms of Use: http://spiedigitallibrary.org/ss/termsofuse.aspx

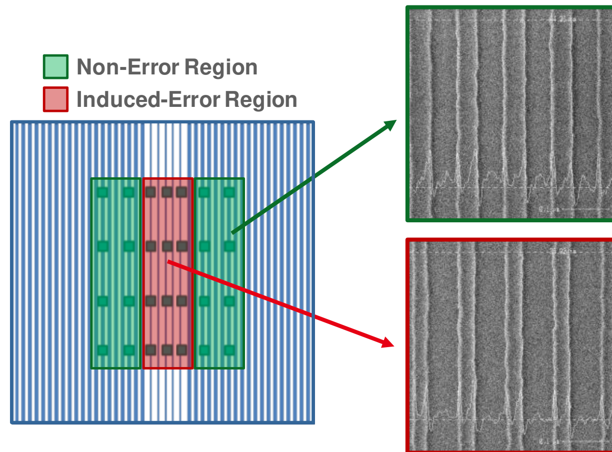

Figure 6: An example of the placement of reference CD-SEM measurement locations within an OCD target. Some of the locations are inside the non-POR region (also called the "error" or "induced-error" region), while some are inside the POR, or "non-error," region. These measurement locations are distributed in an approximately uniform manner where the OCD measurement spot is placed, even though this meant changing the relative number of measurement locations in the error versus the non-error regions. Three lines were measured within each CD-SEM measurement location. Sample CD-SEM images showing the smaller lines of the error region (compared to the non-error region) are provided.

Because OCD measures the average CD across its measurement spot, the average CD from the CD-SEM must properly take into account the contributions from both the non-error and error regions in order for a correct comparison to occur. To do this, the average of the measured CDs from the non-error region $(\overline{CD}_{NE_{meas}})$ and the average of the measured CDs from the error region $(\overline{CD}_{E_{meas}})$ are weighted by area to determine the CD-SEM weighted average CD for the target:

$$CD_{Weighted} = \frac{(A_{NE})(\overline{CD}_{NE_{meas}}) + (A_E)(\overline{CD}_{E_{meas}})}{A_{NE} + A_E} \quad (7)$$

Where A_{NE} is the total area (sum of areas to the left and right of the central error region) of the non-error region within the OCD measurement spot and A_E is the area of the error region within the spot. Figure 7 shows an example of these two regions with a representation of the OCD spot.

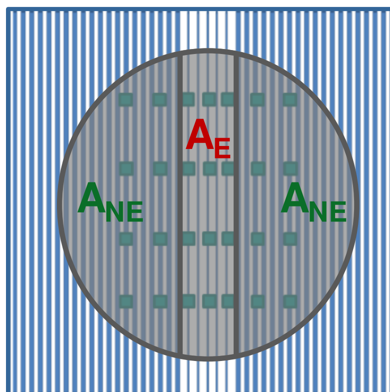

Figure 7: An example of the portions of the non-error (A_{NE}) and error (A_E) regions of an OCD target that are within the representation of the OCD measurement spot. Part of the non-error region is to the left of the error region, and part is to the right of it.

Downloaded From: http://proceedings.spiedigitallibrary.org/ on 04/30/2017 Terms of Use: http://spiedigitallibrary.org/ss/termsofuse.aspx

Because of the non-uniformity of the OCD targets, the calculation of the RMSU (equation 6) also requires care. To take into account the possible difference in variance of the CD between the error and non-error regions of a given target, the variances that are summed in the numerator of equation 6 must also be weighted by area:

$$V_S = (V_S)_{Weighted} = \frac{(A_{NE})((V_S)_{NE}) + (A_E)((V_S)_E)}{A_{NE} + A_E} \quad (8)$$

where $(V_S)_{NE}$ is the variance of the CDs measured in the non-error region of a given target and $(V_S)_E$ is the variance of the CDs measured in the error region. With the assumption that the RMS measurements are evenly distributed throughout the OCD measurement spot, the number n_S of RMS measurements in the denominator of equation 6 should not be weighted—n_S for each sample (target) is the sum of the number of CD-SEM measurements in both the error and non-error regions of that sample. Equation 6 then sums each of these values of n_S across the total number of samples N_S.

4. RESULTS

4.1 OCD Spectra

A straightforward method to confirm OCD's ability to successfully measure the difference in dose variation among the targets is to qualitatively compare their spectra. Figure 8 shows measured spectral variation for three of the dose-shifted targets, as compared to the POR target. As expected, the spectral shift increases with the size of the dose shift and with the increase in the number of beams affected by the dose shift.

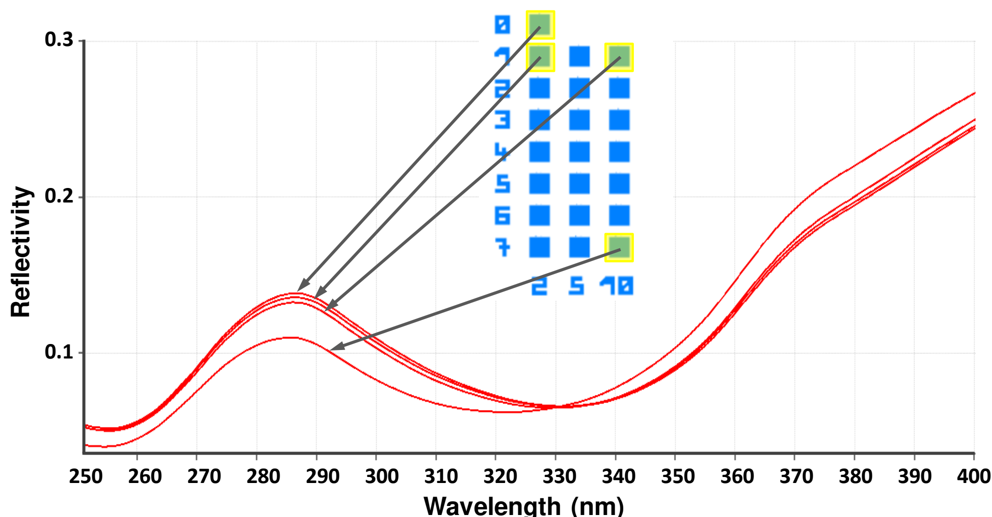

Figure 8: Spectral variation of 3 dose-shifted targets as compared to the POR target, indicating scatterometry's sensitivity to the dose shifts. The spectral shift increases with the mangnitude of the dose shift and the number of beams that have been dose-shifted. To make the spectral variation easier to see, only part of the spectrum is shown (from 250 – 400 nm), and only one of the six OCD spectral channels is displayed—others have similar spectral sensitivities.

4.2 Trends

Another method to assess scatterometry's ability to measure the dose-shifted targets is through the use of trend charts. Figure 9 displays the CD as a function of the number of dose-shifted beams and the magnitude of the dose shift, for (a)

Downloaded From: http://proceedings.spiedigitallibrary.org/ on 04/30/2017 Terms of Use: http://spiedigitallibrary.org/ss/termsofuse.aspx

OCD measurements, (b) estimated CD values, and (c) weighted CD-SEM measurements. The weighted CD-SEM measurements are calculated using equation 7, while the estimated CD values are calculated using

$$CD_{Estimated} = \frac{(A_{NE})(CD_{NE_{nom}}) + (A_E)(CD_{E_{nom}})}{A_{NE} + A_E} \quad (9)$$

where $CD_{NE_{nom}}$ and $CD_{E_{nom}}$ are the nominal (theoretical, or expected) CD values in the non-error and error regions, respectively. The OCD measurements agree well with both the estimated CD values and the weighted CD-SEM measurements, indicating that interpretation of the spectra also provides results that are sensitive to total dose change (magnitude of shift and number of beams).

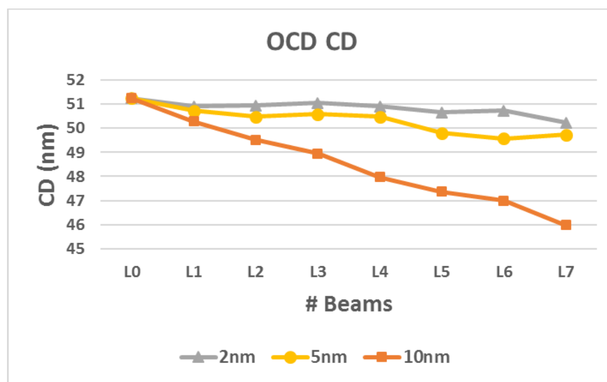

(a)

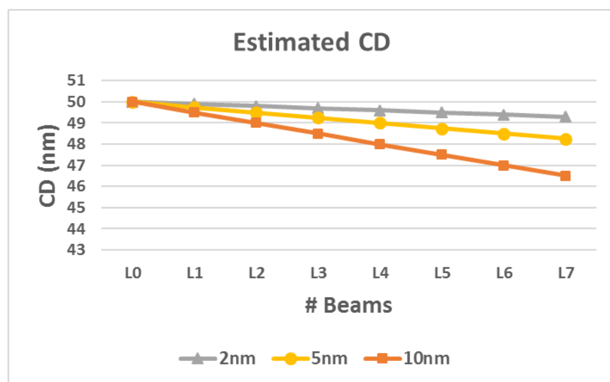

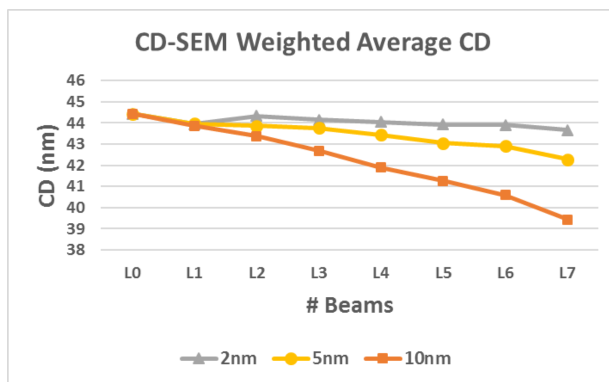

(b) (c)

Figure 9: Trend charts of (a) OCD CD measurements, (b) estimated CD values, and (c) CD-SEM weighted average CD measurements as a function of the number of dose-shifted beams (L0 – L7) and the magnitude of the nominal dose shift measured in nm (2, 5, and 10 nm). The OCD measurements track the other results well.

4.3 Correlation to CD-SEM

As a final method of determining OCD's ability to successfully measure the dose-shifted targets, a correlation to the weighted CD-SEM values is provided in figure 10. These results are from all of the different types of dose-shifted targets, from die across the wafer. The results are quite unexpected, as TMU values for this type of application (line/space resist on a simple film stack) are typically around 1 nm.

Downloaded From: http://proceedings.spiedigitallibrary.org/ on 04/30/2017 Terms of Use: http://spiedigitallibrary.org/ss/termsofuse.aspx

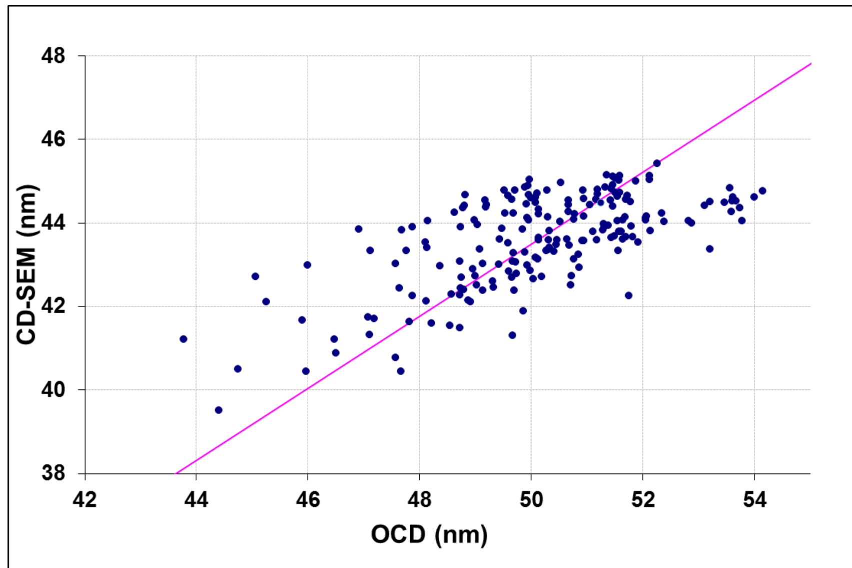

TMU	3.65 nm
R^2	0.44
Slope	0.87
Average Offset	6.5 nm
Data Pairs	197

Figure 10: TMU correlation results across the different dose-shifted targets and die. Explanation for the primary cause of the scatter is provided in the text. "Data Pairs" is the number of data points in the correlation graph.

A partitioning of the results by die found that the individual correlation best-fit line slopes and average offsets vary considerably from one die to the next. This is shown in figures 11 and 12. Upon investigation, it was found that the cause for this variation in slope and offset is from changes in resist morphology due to variation of the resist develop process across the wafer. The changes in resist morphology are significant enough to cause a variation in CD measurement sensitivity between OCD and CD-SEM, resulting in the different slopes and offsets.

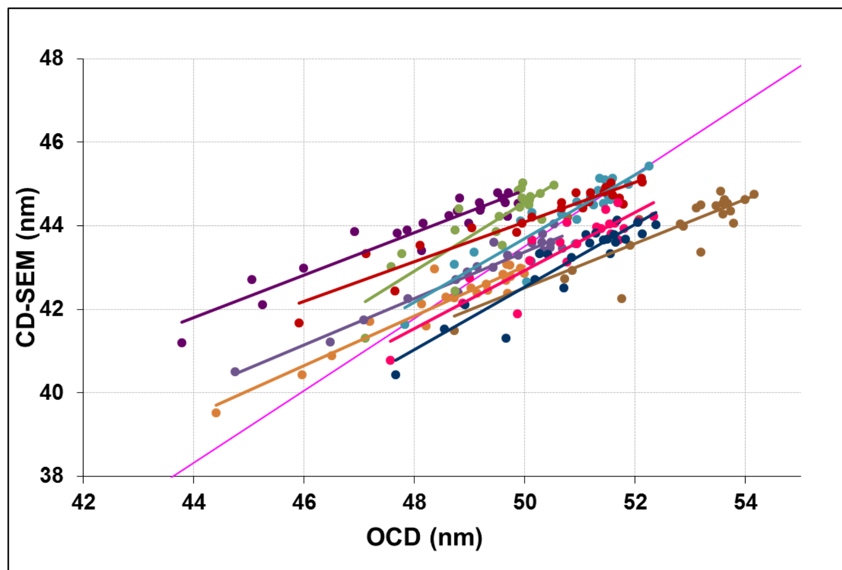

Figure 11: Partitioning of the correlation results by die. Individual best-fit lines for each die, as well as the best-fit line for the entire data set (longest line), are shown and have considerably different slopes and offsets. Each colored group of data points and best-fit line in the correlation graph corresponds to one of the nine colored die in the wafer map shown. For the wafer map the notch is at the bottom position. Explanation for the different slopes and offsets is provided in the text.

Downloaded From: http://proceedings.spiedigitallibrary.org/ on 04/30/2017 Terms of Use: http://spiedigitallibrary.org/ss/termsofuse.aspx

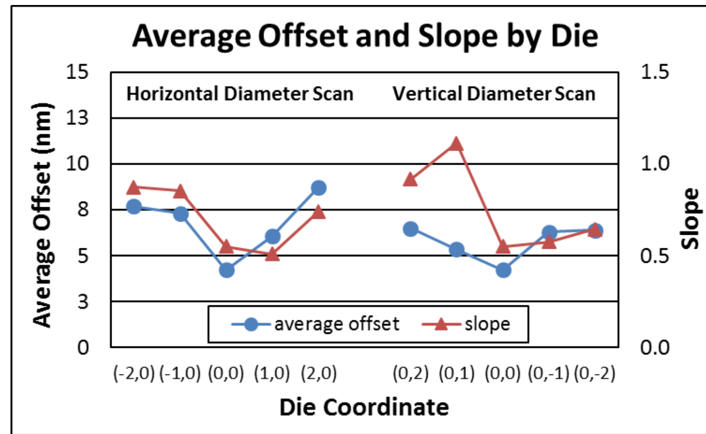

Figure 12: Best-fit line slopes and average offsets of the individual (by die) OCD vs. CD-SEM correlations, shown as horizontal (left side) and vertical (right side) diameter scans. Explanation for the different slopes and offsets is provided in the text.

A re-plotting of the correlation results, this time separating the data by die onto different graphs (figure 13), shows significantly better correlations. Figure 14 shows both the TMU and R^2 results for these individual correlations, plotted as both horizontal and vertical diameter scans. TMU values between 0.5 and 1.7 nm are achieved, which are consistent with expectations and demonstrate scatterometry's ability to successfully measure the dose-shifted targets. Although the R^2 metric is not promoted in this work, such results are shown in order to help those readers not familiar with TMU analysis have a benchmark for comparison.

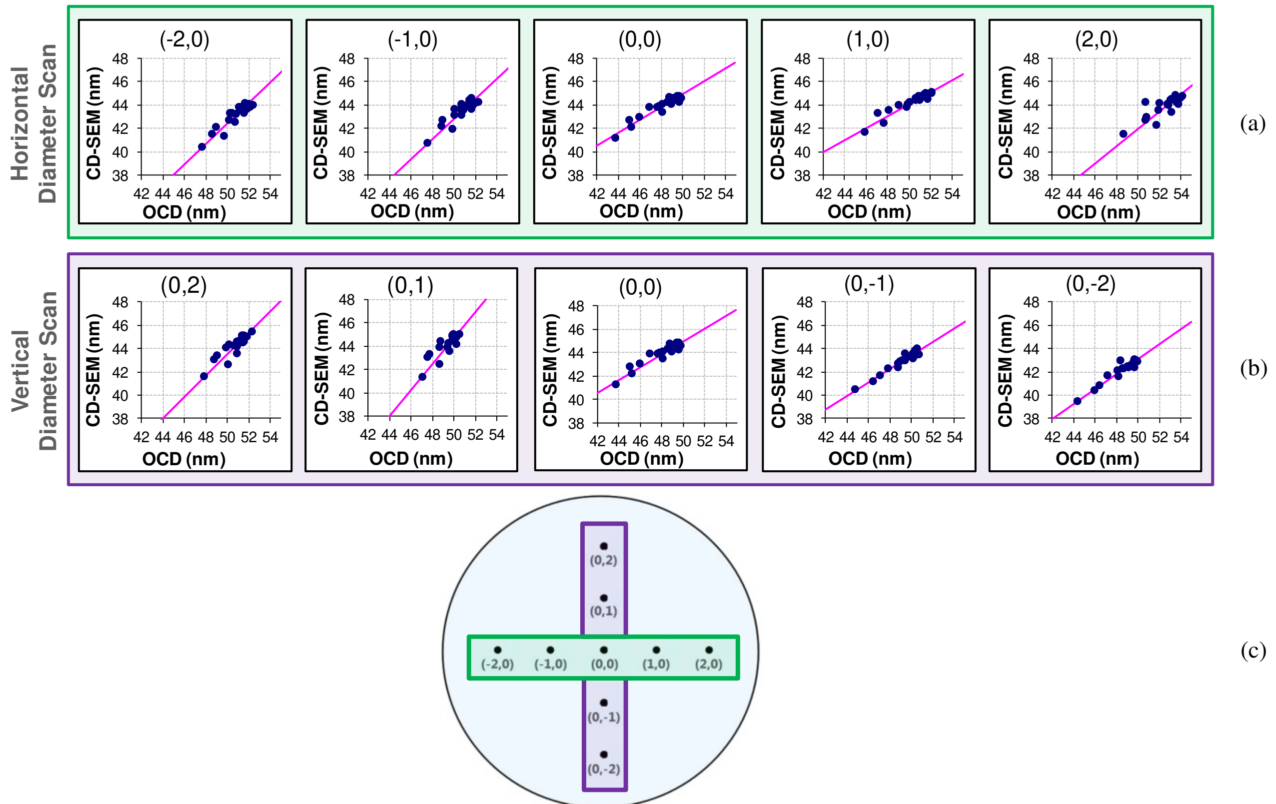

Figure 13: Partitioning of the correlation results into separate graphs: (a) horizontal diameter scan, (b) vertical diameter scan, and (c) wafer map. For the wafer map the notch is at the bottom position.

Downloaded From: http://proceedings.spiedigitallibrary.org/ on 04/30/2017 Terms of Use: http://spiedigitallibrary.org/ss/termsofuse.aspx

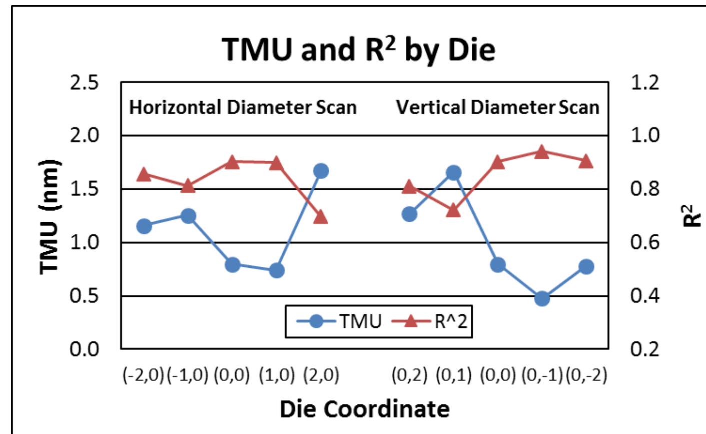

Figure 14: OCD vs. CD-SEM correlation TMU and R^2 results by die. Good correlations are achieved (TMU values range from 0.5 to 1.7 nm).

5. CONCLUSIONS

As the importance of alternative lithography methods increases, so too does the need for having in-line, non-destructive metrology techniques for monitoring and controlling such methods. In this study, specialized scatterometry targets that mimic potential exposure dose errors from a multiple electron beam lithography system are described and used to test the ability of scatterometry to detect such errors. What differentiates these targets is their intentional non-uniformity in CD caused by the intentional within-target dose variations. Traditionally, scatterometry is used to measure nominally uniform targets, but in this work it is discovered that OCD is spectrally sensitive to such variations, and that the resulting OCD measurements successfully track trends produced both by theoretical calculations of CD as well as weighted measurements from CD-SEM. As a final confirmation of scatterometry's ability to track within-target dose variations, direct correlation to CD-SEM is provided and found to be very good after taking into account variations in resist morphology across the wafer. TMU analysis, a methodology more rigorous than Ordinary Least Squares regression, was used to quantify the correlation. TMU values, indicating the combined accuracy and precision error of the OCD measurement, range from 0.5 to 1.7 nm. In order to calculate these TMU values, a new method for estimating the error of the CD-SEM measurements for intentionally non-uniform targets is presented.

REFERENCES

[1] P. Brandt, J. Belledent, C. Tranquillin, T. Figueiro, S. Meunier, S. Bayle, A. Fay, M. Milléquant, B. Icard, M. Wieland, "Demonstration of EDA flow for massively parallel e-beam lithography ", Proc. SPIE 9049, Alternative Lithographic Technologies VI, 904915 (2014); doi:10.1117/12.2046091.

[2] Robin Chao, Chi-Chun Liu, Cornel Bozdog, Aron Cepler, Matthew Sendelbach, Oded Cohen, Shay Wolfling, Todd Bailey, Nelson Felix, "Scatterometry-based Defect Detection for DSA In-line Process Control", Proc. of SPIE Vol. 9424, 942419-1 (2015); doi: 10.1117/12.2087093.

[3] G. de Boer, M. Dansberg, R. Jager, J. Peijster, E. Slot, S. Steenbrink, M. Wieland, "MAPPER: progress toward a high-volume manufacturing system" Proc. SPIE 8680, Alternative Lithographic Technologies V, 86800O (2013); doi: 10.1117/12.2011486.

[4] M. Wieland *et. al.*, "Performance validation of Mapper's FLX-1200", Alternative Lithographic Technologies VII, SPIE, 9423-9434, (2015).

[5] Sendelbach, M., *et. al.*, "Impact of shrinking measurement error budgets on qualification metrology sampling and cost" in *Metrology, Inspection, and Process Control for Microlithography XXVIII*, edited by Jason P. Cain, Proceedings of SPIE Vol. 9050 (SPIE, Bellingham, WA 2014) 90501M.

Downloaded From: http://proceedings.spiedigitallibrary.org/ on 04/30/2017 Terms of Use: http://spiedigitallibrary.org/ss/termsofuse.aspx

[6] Sendelbach, M., Archie, C. N., "Scatterometry measurement precision and accuracy below 70 nm" in *Metrology, Inspection, and Process Control for Microlithography XVII*, edited by Daniel J. Herr, Proceedings of SPIE Vol. 5038 (SPIE, Bellingham, WA 2003) pp. 224-238.
[7] Sendelbach, M., Munoz, A., Bandy, K. A., Prager, D., Funk, M., "Integrated scatterometry in high-volume manufacturing for polysilicon gate etch control" in *Metrology, Inspection, and Process Control for Microlithography XX*, edited by Chas N. Archie, Proceedings of SPIE Vol. 6152 (SPIE, Bellingham, WA 2006) 61520F.
[8] Sendelbach, M., Natzle, W., Archie, C. N., Banke, B., Prager, D., Engelhard, D., Ferns, J., Yamashita, A., Funk, M., Higuchi, F., Tomoyasu, M., "Feedforward of mask open measurements on an integrated scatterometer to improve gate linewidth control" in *Metrology, Inspection, and Process Control for Microlithography XVIII*, edited by Richard M. Silver, Proceedings of SPIE Vol. 5375 (SPIE, Bellingham, WA 2004) pp. 686-702.

Downloaded From: http://proceedings.spiedigitallibrary.org/ on 04/30/2017 Terms of Use: http://spiedigitallibrary.org/ss/termsofuse.aspx